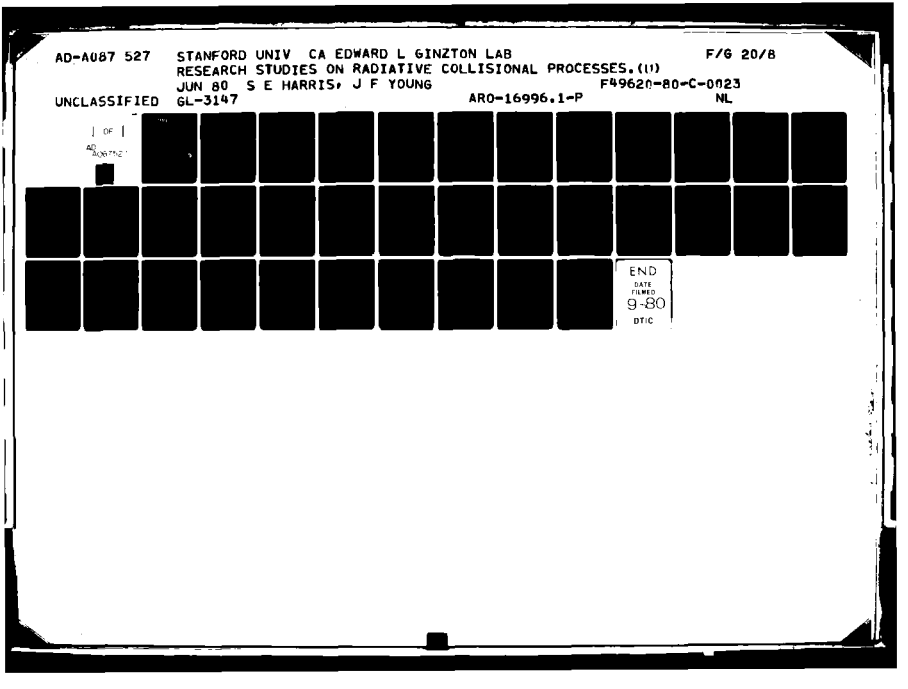
AD-A087 527
STANFORD UNIV CA EDWARD L GINZTON LAB
RESEARCH STUDIES ON RADIATIVE COLLISIONAL PROCESSES.(U)
JUN 80 S E HARRIS, J F YOUNG
F/G 20/8
UNCLASSIFIED
GL-3147
ARO-16996.1-P
F49620-80-C-0023
NL
END
DATE FILMED
9-80
DTIC

Edward L. Ginzton Laboratory
W. W. Hansen Laboratories of Physics
Stanford University
Stanford, California

RESEARCH STUDIES ON RADIATIVE COLLISIONAL PROCESSES

Interim Technical Report

for the period

Beginning October 1979

Sponsored by

Air Force Office of Scientific Research (AFSC)
United States Air Force

and

Army Research Office
United States Army
Under Contract F49620-80-C-0023

Co-Principal Investigators - Professors S. E. Harris and J. F. Young

G.L. Report No. 3147

UNCLASSIFIED

SECURITY CLASSIFICATION OF THIS PAGE (When Data Entered)

REPORT DOCUMENTATION PAGE		READ INSTRUCTIONS BEFORE COMPLETING FORM
1. REPORT NUMBER	2. GOVT. ACCES. NO. AD-A087527	3. RECIPIENT'S CATALOG NO.
4. TITLE (and Subtitle) Research Studies on Radiative Collisional Processes		5. TYPE OF REPORT Interim Special Technical Report,
		6. PERFORMING ORG'N REPORT NO. G.L. Report No. 3147
7. AUTHOR(S) S. E. Harris J. F. Young		8. CONTRACT OR GRANT NO. F49620-80-C-0023
9. PERFORMING ORG'N NAME AND ADDRESS Edward L. Ginzton Laboratory Stanford University Stanford, California 94305		10. PROGRAM ELEMENT, PROJECT, TASK AREA & WORK UNIT NUMBERS
11. CONTROLLING OFFICE NAME AND ADDRESS Air Force Office of Scientific Research Bolling Air Force Base Washington, D. C. 20332		12. REPORT DATE June 1980
		13. NO. OF PAGES 33
14. MONITORING AGENCY NAME & ADDRESS(if different from 11. above)		15. SECURITY CLASS (of this report) Unclassified
		15a. DECLASSIFICATION DOWNGRADING SCHEDULE
16. DISTRIBUTION STATEMENT (of this Report) Approved for Public Release Distribution Unlimited		
17. DISTRIBUTION STATEMENT (of the Abstract entered in Block 20, if different from Report)		
18. SUPPLEMENTARY NOTES THE VIEW, OPINIONS, AND/OR FINDINGS CONTAINED IN THIS REPORT ARE THOSE OF THE AUTHOR(S) AND SHOULD NOT BE CONSTRUED AS AN OFFICIAL DEPARTMENT OF THE ARMY POSITION, POLICY, OR DECISION, UNLESS SO DESIGNATED BY OTHER DOCUMENTATION.		
19. KEY WORDS (Continue on reverse side if necessary and identify by Block no.) Radiative Collisional Processes Ground State (of an Ion)		
20. ABSTRACT (Continue on reverse side if necessary and identify by Block no.) A radiative collisional process is one wherein two atoms and a photon simultaneously participate. In the prototype reaction, energy is first stored in a state of some atom and an incident laser is tuned so as to satisfy the energy defect between this storage state and a selected state of a second atom. In the presence of this incident laser beam, the collision cross section may be as large as 10^{-12} cm^2 (i.e., corresponding to billiard ball size of the atoms of almost 100 Å), thereby allowing		

EDITION OF 1 NOV 65 IS OBSOLETE

DD FORM 1 JAN 73 1473

409 640

UNCLASSIFIED

SECURITY CLASSIFICATION OF THIS PAGE (When Data Entered)

rapid transfer of energy to the target species.

Of particular interest, the storage species may not only be an excited state of an atom, but instead may also be the ground state of an ion. An intense laser field may then be used to rapidly transfer this energy to an excited ionic state of a second species. Such a process is termed as laser induced charge transfer. Since ground state ions are easily created and represent a means of long-lived energy storage, laser induced charge transfer processes are particularly exciting for applications.

If the storage state of the first atom is at higher energy than that of the target state of the second atom, then an incident laser photon will experience gain rather than loss; and stimulated emission may occur at a characteristic frequency equal to the difference of the energy levels of the two species. In the visible, the gain linewidth for such a dipole-dipole laser will be a few angstroms. The gain cross section will be quite low, but once stimulated emission is obtained, the energy storage will be very high.

An interesting and initially unexpected process that has arisen during the course of our work on radiative collisional processes is termed as atomic pair absorption. In such a process an incident laser photon tuned to the sum energy of two different atomic species simultaneously populates both species. During the first six months of this contract we have demonstrated for the first time the use of such a process to obtain a laser in one of the species. Of particular interest, Falcone has suggested that pair absorption processes may be used to invert atomic species with regard to their ground energy levels. For example, radiation from a KrF laser at 2480 Å incident on a mixture of Li and K could, depending on the densities of the two species, cause the inversion of the K resonance line or the Li(3s-2s) nonallowed storage level. In the latter case the accumulated energy could be extracted in a short burst by a stimulated Raman process.

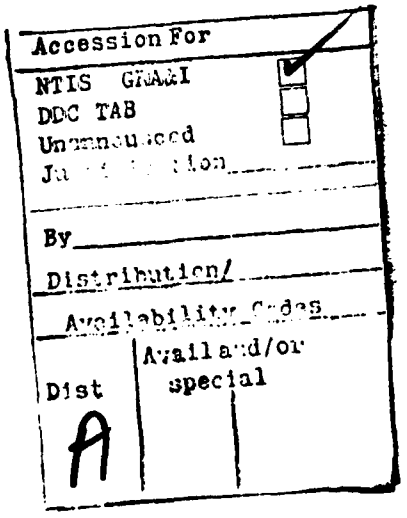

EXTRACTED FROM PROPOSAL DATED JUNE 1980

II. SUMMARY OF PROGRESS TO DATE

A. Laser Induced Charge Transfer

(M. D. Wright and D. M. O'Brien)

In the past year, we have conducted the first experimental observations of laser induced charge transfer collisions. The particular reactions studied are

$$Ca^{+}(4s\ ^{2}S_{1/2}) + Sr(5s^{2}\ ^{1}S_{0}) + \hbar\omega(4715\ \text{Å}) \rightarrow Ca(4s^{2}\ ^{1}S_{0}) + Sr^{+*}(5p\ ^{2}P^{o}_{3/2}) \quad (1)$$

$$Ca^{+}(4s\ ^{2}S_{1/2}) + Sr(5s^{2}\ ^{1}S_{0}) + \hbar\omega(4800\ \text{Å}) \rightarrow Ca(4s^{2}\ ^{1}S_{0}) + Sr^{+*}(5p\ ^{2}P^{o}_{1/2}) \quad (2)$$

These reactions are depicted schematically in Fig. 1. In both collision systems, the applied laser photon raises one of the two Sr valence electrons to a virtual state of $Sr(5s5p\ ^{1}P^{o}_{1})$ character. As the Sr atom in a virtual state collides with a Ca^{+} ion, the remaining unexcited Sr valence electron is transferred to the Ca^{+} ion, leaving a Ca ground state neutral and an excited Sr^{+*} ion.

Our studies of the reactions given by Eq. (1) and (2) have established some interesting differences between these two collision systems. For the reaction described by Eq. (1), the charge transfer cross section maximizes when the applied laser photon is tuned to 4715 Å which is ~ 70 cm^{-1} more

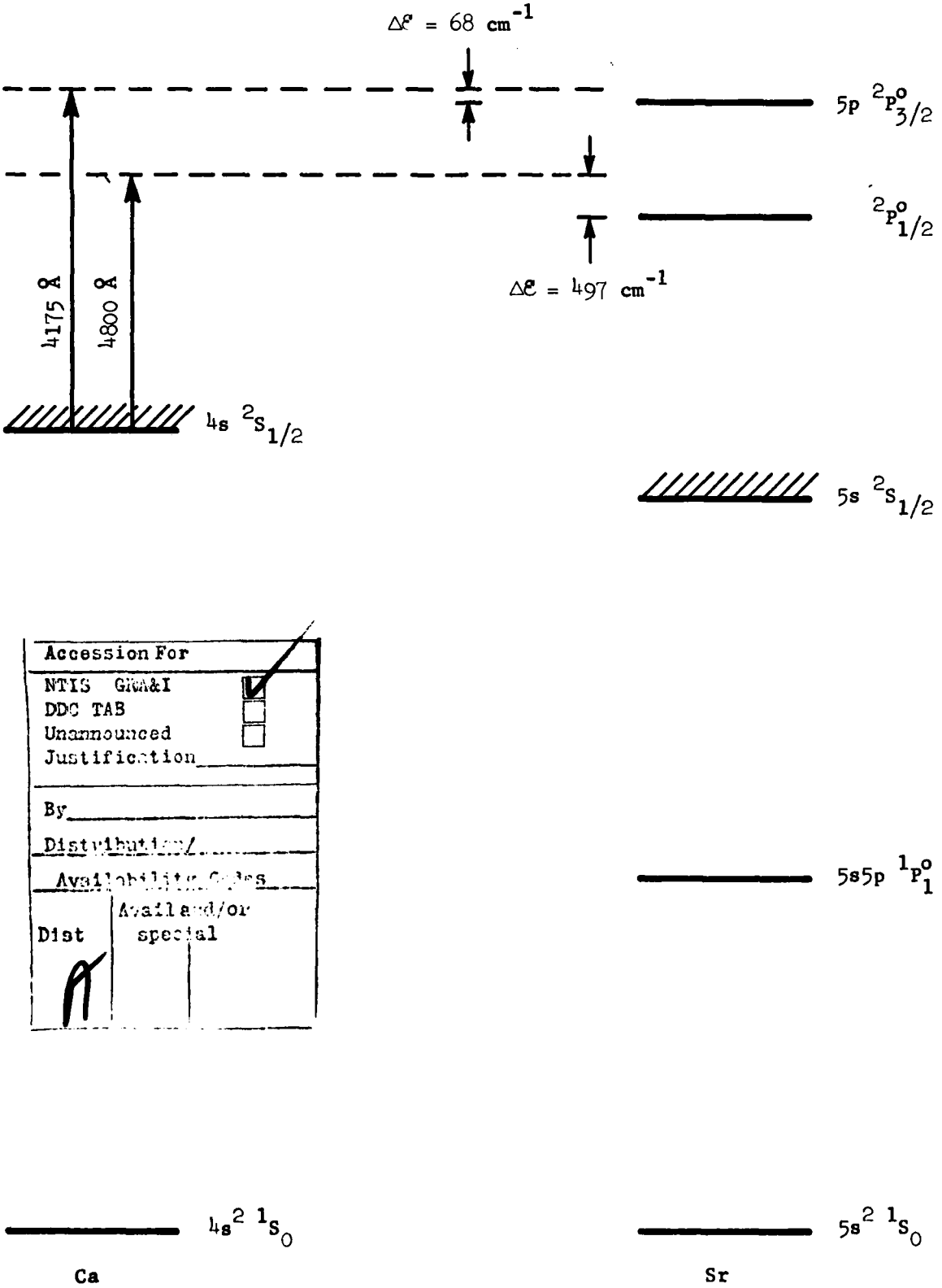

Fig. 1--Energy level diagram for Ca-Sr laser induced charge transfer collisions.

energetic than the photon which is required to exactly satisfy the energy defect of Eq. (1) when the colliding species are infinitely separated; the linewidth of the cross section is ~ 50 cm^{-1}. At an applied laser power density of 10^8 W/cm^2, the peak cross section for Eq. (1) is estimated to be 2×10^{-15} cm^2. For the reaction described by Eq. (2), the charge transfer cross section maximizes when the applied laser photon is tuned to 4800 Å which is ~ 500 cm^{-1} more energetic than the $\lambda_{R=\infty}$ photon; also, the linewidth of the cross section is ~ 325 cm^{-1}. At an applied laser power density of 10^8 W/cm^2, the peak cross section for Eq. (2) is estimated to be 2×10^{-16} cm^2.

The above described differences in the systems given by Eqs. (1) and (2) may be partially understood upon consideration of the potential energy curves associated with these collision reactions. The potential energy curves for the initial and final states of Eq. (1) are nearly parallel due to nearly equal C_4's for Sr and Ca. The potential energy curves for the initial and final states of Eq. (2) are not parallel, however, due to the influence of a nearly resonant C_6 arising from the dipole-dipole interaction between Ca and $Sr^{+*}(5p\ ^2P^o_{1/2})$. Hence, the cross section peak may be expected to be more significantly displaced from the $\lambda_{R=\infty}$ wavelength in the reaction given by Eq. (2) than in the reaction given by Eq. (1); also, the lineshape associated with Eq. (2) should be broader than that associated with Eq. (1). The smaller value for the peak cross section of Eq. (2) relative to that of Eq. (1) is due to a greater detuning of the applied laser photon with respect to the $Sr(5s5p\ ^1P^o_1)$ intermediate state.

Our efforts to experimentally demonstrate laser induced charge transfer collisions have proven successful, and the particular systems we have studied have provided much insight into the physics of the process.

B. Pair Absorption Pumped Lasers

(R. W. Falcone and G. A. Zdasiuk)

During the report period we have demonstrated the use of a novel optical pumping technique based on atomic pair absorption as a practical means of populating atomic energy levels. Pair absorption refers to a process in which two collidng atoms simultaneously absorb a single photon at a frequency corresponding to the sum energy of levels in the separated atoms. By the use of intense laser sources we have found that it is possible to construct atomic pair absorption pumped lasers.

The system used for our experiments is shown in Fig. 2. Here, Ba and Tℓ atoms collide and absorb a photon at $\lambda = 3867$ Å. After the collision, the Tℓ atom is left in a $6p\ ^2P^o_{3/2}$ state and the Ba atom in the $6p\ ^1P^o_1$ resonance level. If the pumping rate (as determined by the $\lambda = 3867$ Å photon flux and the atomic number densities) is sufficient, there will be a population inversion between the Ba $6p\ ^1P^o_1$ and $5d\ ^1D_2$ levels and subsequent superfluorescent laser emission at $\lambda = 1.5$ μm.

Our preliminary results indicate that for $N_{Ba} \sim 4 \times 10^{17}/cm^3$ and $N_{T\ell} \sim 1.7 \times 10^{17}/cm^3$, the threshold pumping power at $\lambda = 3867$ Å for lasing on the 1.5 μm transition is $\sim 5 \times 10^5$ W/cm^2. The resulting inversion density ($N_{Ba}\ 6p\ ^1P^o_1 - N_{Ba}\ 5d\ ^1D_2$) is greater than 10^{14} atoms/cm^3. Figure 3 shows the relative intensity of the $\lambda = 1.5$ μm laser as a function of the pumping wavelength. This can be compared with the white light absorption scan taken under similar operating conditions shown in Fig. 4. The scans indicate that both the absorption spectrum and laser pumping wavelength dependence have similar lineshapes, as would be expected.

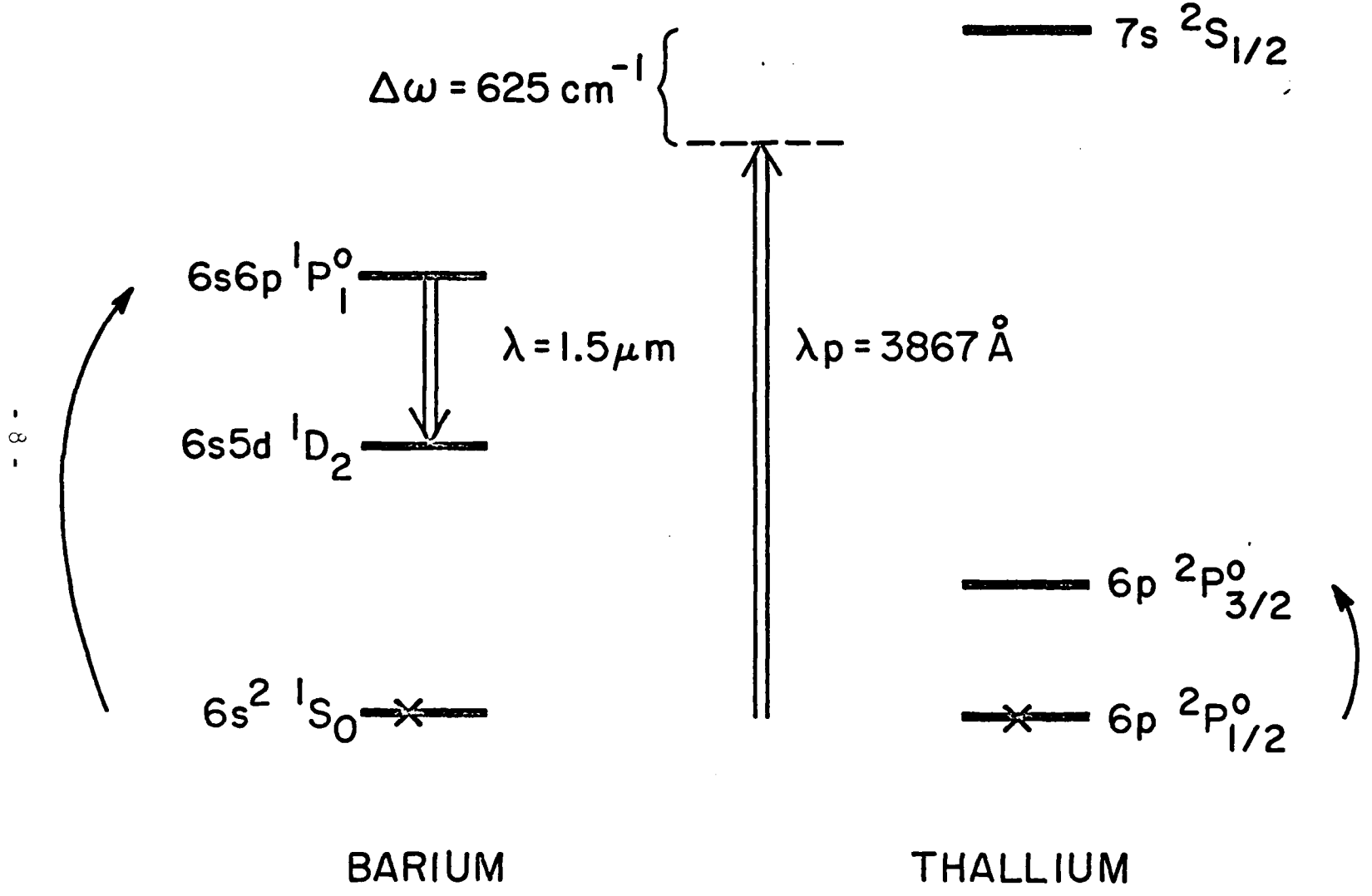

Fig. 2--Pertinent Ba and Tℓ levels for the pair absorption pumped laser. During the collision of a Ba atom with a Tℓ atom, a photon is absorbed at 3867 Å, resulting in the simultaneous excitation of the Ba atom to the 6p $^1P^o_1$ level and the Tℓ atom to the 6p $^2P^o_{3/2}$ level. If the pumping rate is sufficient, superfluorescent laser action will occur on the Ba 6s6p $^1P^o_1$ - 6s5d $^1D_2$ transition at λ = 1.5 μm .

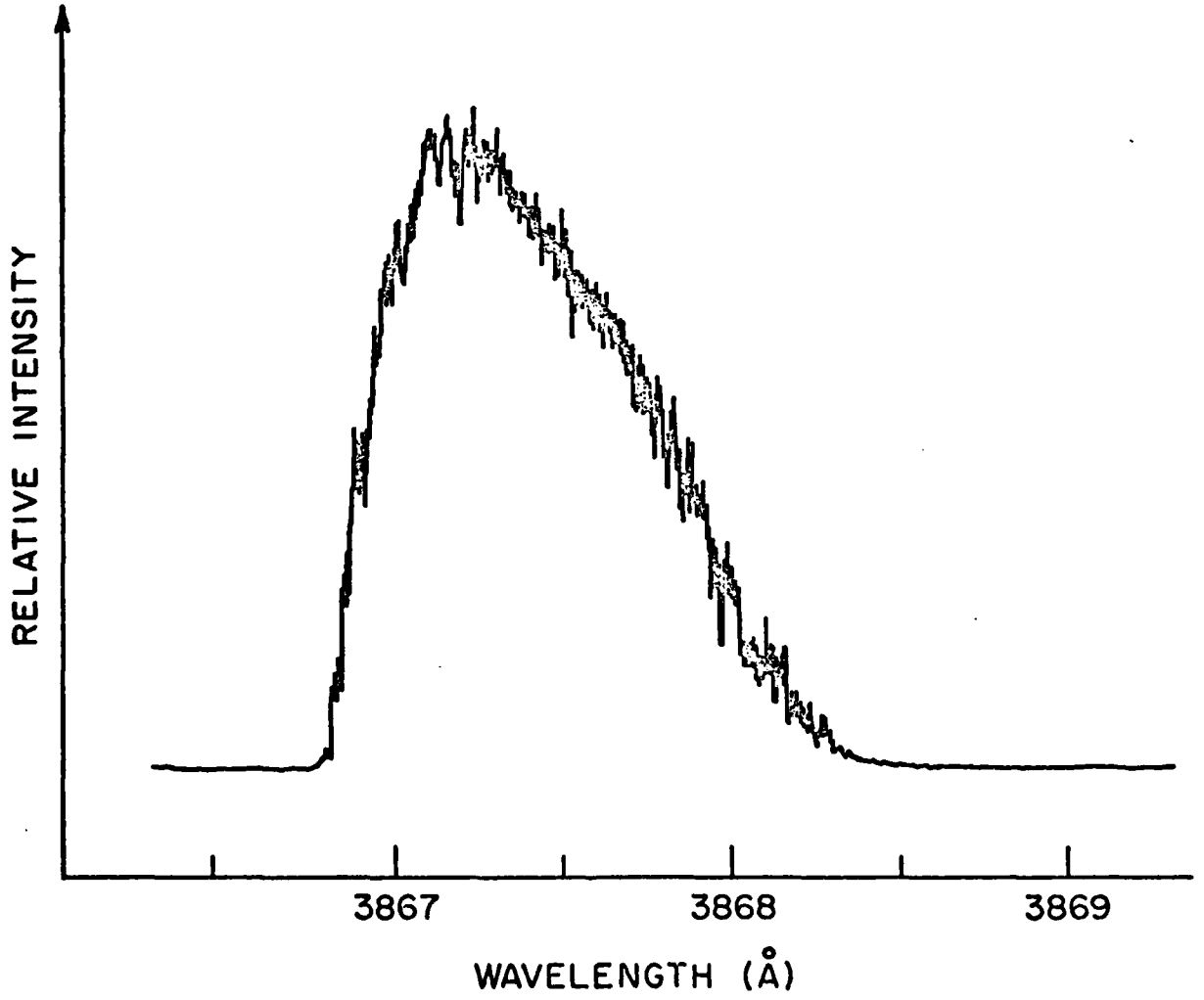

Fig. 3--Relative intensity of the $\lambda = 1.5$ μm laser as a function of pumping wavelength. The intensity maximizes at the predicted wavelength of 3867 Å and the profile asymmetry is similar to that of the white light absorption scan (see Fig. 4).

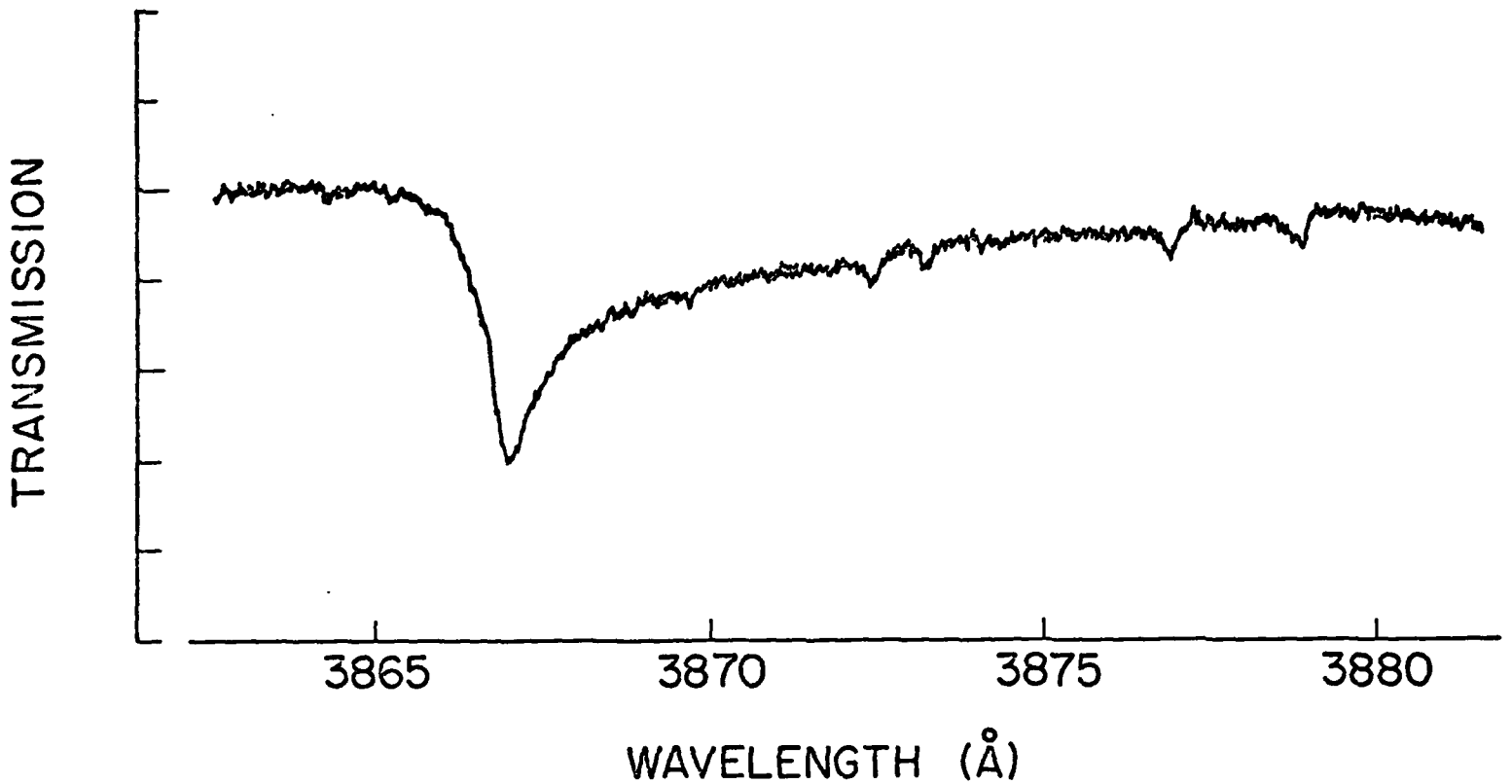

Fig. 4--White light absorption scan showing the Ba-Tl pair absorption feature at 3867 Å.

In the coming contract period we propose expanding our work on optically pumped pair absorption lasers. In particular, we plan to invert a metal vapor species with respect to its ground state. This goal seems achievable in light of our recent experimental verification of this pumping technique in producing the first pair absorption pumped Ba laser. In that experiment the inversion was not to the ground state, but was on the upper level transition $Ba(6s6p\ ^1P_1^o - 6s5d\ ^1D_2)$. In order to invert a species to the ground state, the pumping laser must drive the pair absorption reaction $A^o + B^o + \hbar\omega \rightarrow A^* + B^*$ such that more than half of the initial concentration of ground state atoms A^o are converted to excited A^*. This will occur in the presence of both a high density of species B^o and sufficient laser power density at a photon energy $\hbar\omega$ equal to the sum energy of the excited states A^* and B^*.

Inversion to ground state on the transition $A^* \rightarrow A^o$ has several applications which we plan to explore. The first is resonance line lasers, if the transition is dipole allowed. Resonance line lasers may be useful for isotope separation and for trace analysis and detection. If the transition is (dipole) nonallowed, inversion to the ground state may allow development of two photon and Raman anti-Stokes lasers since large energy densities could be stored in these metastable states. One application of this technique would be the temporal and wavelength compression of high powered excimer lasers. Absorption of the relatively broadband excimer radiation into a specific storage state of a target species would be accomplished by selecting the appropriate second species for the pair absorption process. The density of this second species, and equivalently, the pair absorption cross section, would be chosen to cause inversion to ground of the target species by the end of the excimer

laser pulse. Rapid extraction of the stored energy could then be effected by Raman, two photon, or other lasing process between the target state and the empty ground state. Several proposed pair absorption systems which could absorb the currently available high powered excimer laser wavelengths are given in Table 1.

Our initial experiments to observe inversion to ground by pumping pair absorption transitions will involve one of the metal vapor systems listed in Table 2. These systems have been selected for both their useful excited states and strong pair absorption cross sections. These absorption cross sections are typically > 1 Å bandwidth, thus allowing the use of relatively broadband laser pumping sources. Typical energy density requirements for inversion to the ground state as 1 joule/cm^2 applied at the pump wavelength indicated. One aspect of the pair absorption process which must be studied experimentally is the effect of possible stimulated Raman-Stokes emission generated in one species by the pump laser. This was not a problem in the optically pumped Ba laser system we investigated, but may be more serious at the high pump laser powers required to invert species to the ground state. If the dipole-quadrupole interaction is used as the collisional coupling mechanism between colliding species in the pair absorption, this potential problem can be avoided. This type of coupling is illustrated by experiments 3 and 4 of Table 2. It has recently been shown in our laboratory that dipole-quadrupole induced collision processes can be as strong as dipole-dipole interactions.

In addition to inverting a prototype metal vapor system to the ground state by pumping pair absorption transitions, we hope to identify the potential of such techniques for making new types of useful optically pumped

Table 1

Excimer Laser Pumped Pair Absorption Systems

Excimer Laser Pump	Wavelength (nm)	States Excited in Pair Absorption System	
		Species A	Species B
KrF	248	Li ($3s\ ^2S_{1/2}$)	K ($4p\ ^2P_{3/2}$)
XeF	353	Ba ($5d\ ^1D_2$)	Na ($3p\ ^2P_{1/2}$)
ArF	193	Tℓ ($6p\ ^2P_{3/2}$)	Cd ($6p\ ^1P_1$)
XeCℓ	308	Pb ($6p\ ^3P_2$)	Mg ($3p\ ^3P_1$)
KrCℓ	222	Sr ($4d\ ^1D_2$)	K ($5p\ ^2P_{3/2}$)
XeBr	282	Tℓ ($6p\ ^2P_{3/2}$)	Yb ($5d\ ^1D_2$)

Table 2

Prototype Laser Pumped Metal Vapor Pair Absorption Systems

for Inversion to the Ground State

Experiment	Laser Pump Wavelength	State Excited in Pair Absorption System		Type of Collisional Interaction
		Species A	Species B	
1	3022 Å	Ba($6s5d\ ^1D_2$)	Sr($5s5p\ ^1P^o_1$)	dipole/dipole
2	4182 Å	Sr($5s5p\ ^1P^o_1$)	In($5p\ ^2P^o_{3/2}$)	dipole/dipole
3	2854 Å	Ba($6s6p\ ^1P^o_1$)	Na($3p\ ^2P^o_{3/2}$)	dipole/quadrupole
4	3238 Å	Ba($6s6p\ ^1P^o_1$)	Rb($5p\ ^2P^o_{3/2}$)	dipole/quadrupole

atomic and molecular lasers. The practicality of such systems depends in large part on coincidences between useful laser wavelengths and the many new absorption wavelengths created by mixing different species together to form pair absorption systems.

C. Radiative Collisional Fluorescence

(R. W. Falcone and G. A. Zdasiuk)

During the past report period we have made the first observation of radiative collisional fluorescence from thermally excited atoms. This work is also the first observation of such emission from two different atomic species. Previous measurements of radiative collisional fluorescence were made in systems with large atomic excited state populations produced by laser pumping. In our recent work we have found that thermally excited states in hot metal vapor cells result in sufficient excited state populations to produce radiative collisional or pair emission at an intensity which is comparable to that of atomic emission lines.

Figure 5 shows an energy level diagram of the system under consideration. A mixture of Ba and Tℓ metal vapors is contained in a high temperature oven ($T \sim 1700^{\circ}C$). Thermal equilibrium produces a Boltzmann distribution of populations, resulting in $\sim 1 \times 10^{12}$ atoms/cc in the $Ba(6s6p\ ^1P_1^o)$ state and $\sim 2 \times 10^{15}$ atoms/cc in the $T\ell(6p\ ^2P_{3/2})$ state. During a collision the excited Ba and Tℓ atoms simultaneously de-excite and emit a photon by the radiative collisional process

$$Ba^*(6s6p\ ^1P_1^o) + T\ell^*(6p\ ^2P_{3/2}) \rightarrow Ba(6s^2\ ^1S_0) + T\ell(6p\ ^2P_{1/2}) + h\nu(3807\ \text{Å})$$

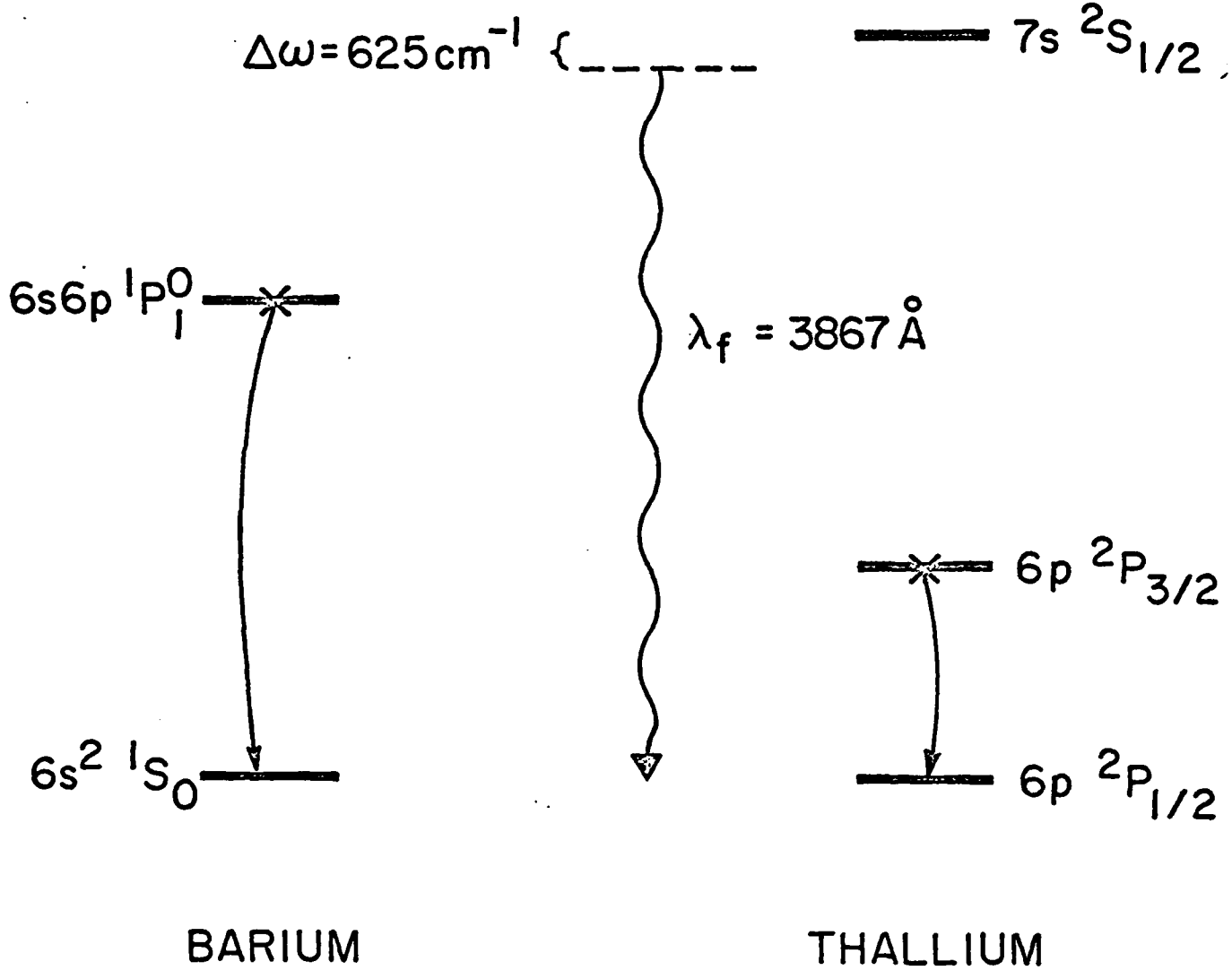

Fig. 5--Energy level diagram for Ba-Tℓ pair emission.

The emitted photon has a wavelength corresponding to the sum energy of the $Ba(6s6p\ ^1P_1^o)$ and the $Tl(6p\ ^2P_{3/2})$ states. Figure 6 shows the observed emission spectrum [Fig. 6(a)] along with a white light absorption scan [Fig. 6(b)] in the same spectral region. The emission profile has an asymmetry to longer wavelengths which is predicted from consideration of the interaction potential of colliding atoms. The absorption scan [Fig. 6(b)] indicates that the cell is nearly optically dense at the absorption transitions indicated. Therefore, all emission lines shown in Fig. 6 are expected to have a characteristic brightness approaching the brightness of a blackbody at the local temperature of the radiating gas as given by the Planck function.

This experiment has demonstrated that radiative collisional emission processes can be studied using simple fluorescence detection apparatus. Emission studies will complement pair absorption studies, especially those involving collisions between highly excited atoms, since fluorescence can be a much more sensitive technique for monitoring small population densities. In our experiment hot wall emission provided a large background noise signal; however, in an electric discharge, atomic populations and subsequent line emission can reflect the electron temperature (which can approach several eV in a hollow cathode, for example) while the discharge walls remain cool. This should provide a relatively noise-free background for studying lineshapes and intensities of radiative collisional processes. Such studies should prove useful in determining intermolecular potentials of colliding atoms and in analyzing new radiative collisional processes.

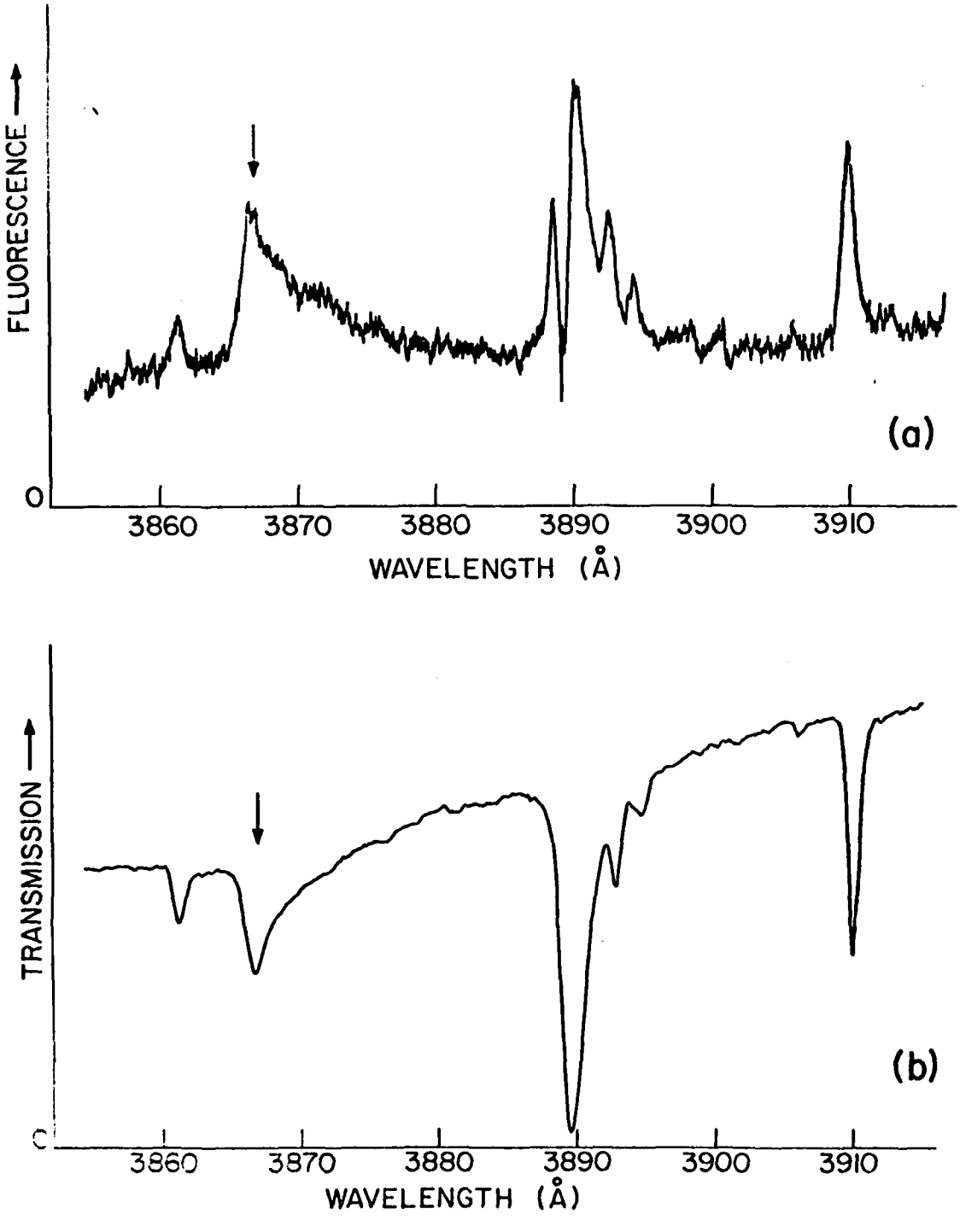

Fig. 6--(a) Fluorescence from Ba-Tℓ metal vapor cell with radiative collisional emission wavelength indicated by arrow.
(b) Absorption of Ba-Tℓ metal vapor cell with pair absorption feature indicated by arrow.

D. Dipole Collision Lasers

(G. A. Zdasiuk)

We are currently evaluating potential systems for constructing dipole-dipole collision lasers. Presently under experimental investigation is an In-Ca switched Collision laser system shown in Fig. 7. The system operates in the following manner. Population is initially stored in the In $5p\ ^2P_{3/2}$ metastable level. This population is then transferred to the Ca $4p\ ^1P_1^o$ level during the collision of a Ca atom with an In atom in the presence of a radiation field at $\lambda = 4665$ Å, corresponding to the energy difference between the Ca $4p\ ^1P_1^o$ level and the In $5p\ ^2P_{3/2}$ state. Subsequent laser emission should occur on the Ca $4p\ ^1P_1^o - 3d\ ^1D$ transition at 5.5 μm. Since the In $5p\ ^2P_{3/2}$ level is only 2213 cm^{-1} above the ground state, significant population (~ 30% of the ground state $5p\ ^2P_{1/2}$ population at cell temperatures of 1700°C) will be present in the level due to thermal excitation. Hence the experiment is very simple, requiring only a single transfer laser, rather than lasers for both pumping the initial state and transferring to the target state. To date, we have attempted to pump the InCa switched collision transition with 4665 Å radiation. We have measured enhancements in the Ca $4p\ ^1P^o$ population; however, no laser emission has been observed on the Ca 5.5 μm line. Laser emission has been observed on various lines in the vicinity of 1.9 μm and 3.9 μm. These laser emission lines are only present when the pump laser is tuned to the vicinity of the switched collision wavelength at 4665 Å, and have intensity vs. pump wavelength profiles which are similar to those obtained with the Ba-Tℓ pair absorption pumped laser. Since we are currently unable to accurately measure these infrared

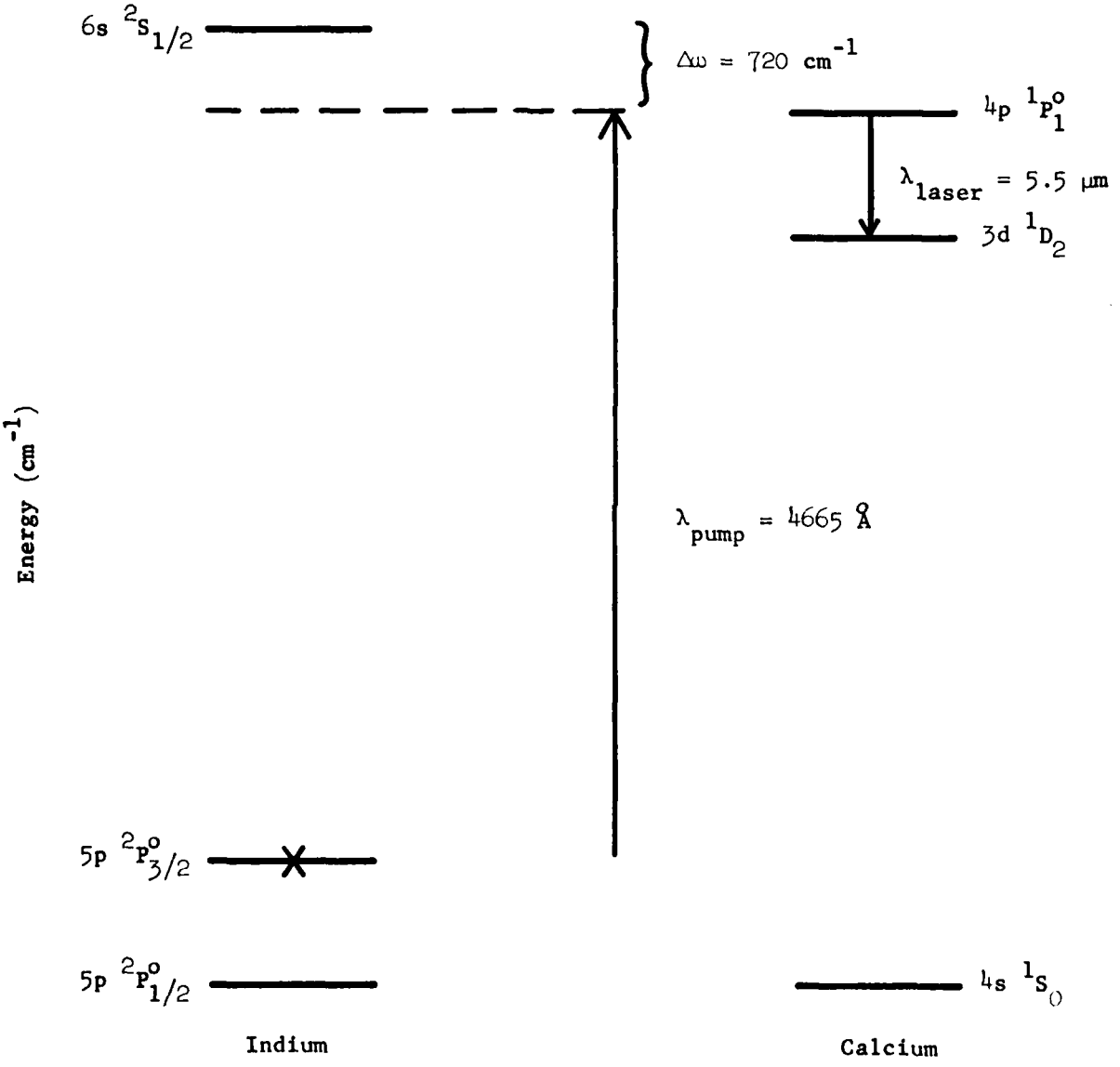

Fig. 7--Indium-calcium switched collision laser.

wavelengths, positive identification of the lasing transitions is not possible. However, our preliminary measurements indicate that the laser action is probably taking place between various states in the Ca triplet manifold. We are attempting to understand the observed behavior and considering the implications for future switched collision lasers.

E. Laser Induced Collision Processes in the Inert Gases

(D. M. O'Brien)

A laser induced collision between Xe and Kr has been attempted, as yet without success. The process (Fig. 8) can be written

$$\text{Xe } 6s'[1/2]_1^o + \text{Kr } 4p^6\ {}^1S_0 + \hbar\omega(6612.6\ \text{Å}) \rightarrow$$
$$+ \text{Xe } 5p^6\ {}^1S_0 + \text{Kr } 5p[5/2]_2 \qquad (3)$$

This system was selected in favor of the previously proposed Xe-Ar collision for two reasons: (1) the oscillator strengths of the pertinent transitions are stronger, resulting in a cross section for collisional transfer that is larger by a factor of six, and (2) the storage state in Xe ($6s'[1/2]_1^o$) is lower in energy and, hence, has a lower threshold for electron excitation from the ground state.

The two most probable causes for the failure of the process of Eq. (3) are: (1) insufficient laser energy, and (2) inadequate storage state (Xe $6s'$) population. The first problem was corrected by switching from a homemade dye laser to a commercial Quanta-Ray system with ten times the output energy. The second problem was attacked by running the discharge at lower total pressure (~ 200 μ as opposed to 5 torr). The lower pressure results in

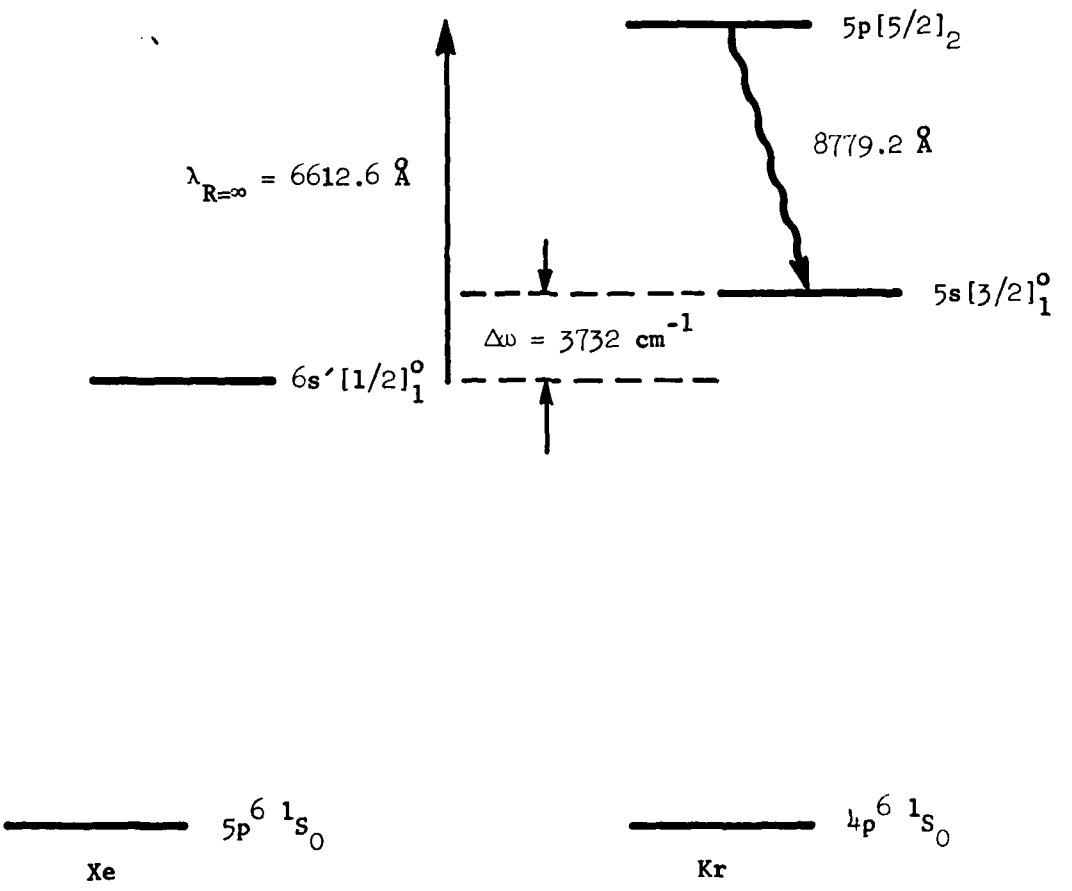

Fig. 8--Xe-Kr laser induced collision.

hotter electrons and hence more population in the resonance lines of Xe. This conclusion was supported by probing the $6s[3/2]^o_1$ resonance line of Xe while changing the pressure. The $6s[3/2]$ and $6s'[1/2]$ levels are separated by ~ 9100 cm^{-1} which should not cause appreciable population differences since both lines are radiatively trapped and, hence, effectively metastable.

The experiment was run once again with initially negative results; however, the discharge cell was damaged by the high laser intensities before conclusive results were obtained. At the present time, the cell has been repaired and a calibration of the optical collection system has been performed. Initial work indicates that we have $\sim 10^9$ cm^{-3} Xe $6s'[1/2]^o_1$ storage state atoms. As anticipated, this rather low storage density makes signal detection difficult. It is possible that with appropriate focusing, etc., the collision process may be observed. Also, the addition of He may increase the electron temperature and, hence, the storage population, as it does in the He-Xe laser. We plan to try again immediately.

An enticing alternative to working in a glow discharge is the afterglow of a pulsed microwave discharge. In the afterglow it is possible to achieve large storage densities through the process of recombination. Further, the microwaves will ionize only those atoms within a skin depth of the outside of the plasma. This makes it possible to have large numbers of ions as well as large numbers of neutrals. After the microwave pulse the ions on the outside diffuse toward the central region, which is composed mainly of neutrals. Thus, we have the possibility of a charge exchange laser as illustrated in Fig. 9. He ions created on the outside diffuse toward the center of the plasma undergoing charge exchange collisions to the $6s\ ^4P_{3/2}$ state of the Xe ion. The cross section for this process is

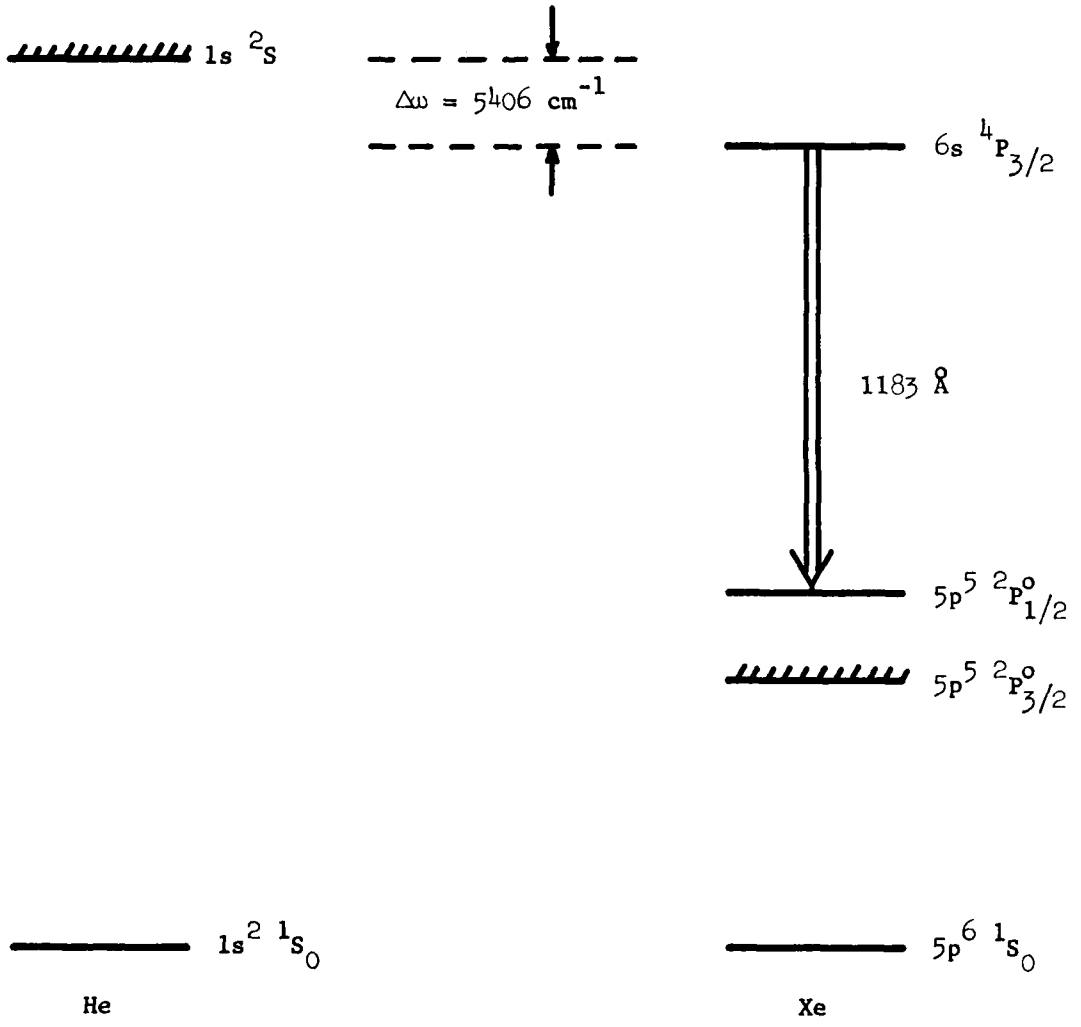

Fig. 9--He-Xe charge exchange laser.

calculated to be $\sim 10^{-15}$ cm^2. If we assume 10^{15} He ions and 10^{16} Xe neutrals, we obtain a collisional rate of 1.5×10^{21} sec^{-1}, which implies a gain of e^4 per cm. This analysis assumes that the lower laser level (Xe $5p^5\ ^2P^o_{1/2}$) is empty. Alternatively, we could require that the rate out of the lower laser level be larger than the rate out of the upper laser level. The dominant rate out of the lower laser level is that due to electron collisions. If we assume a de-excitation cross section of 10^{-14} cm^2, by analogy with He spin exchange cross sections, we find a rate out of 10^9 sec^{-1} for the lower level. Since Xe II is isoelectronic to neutral iodine we can get a clue to the lifetime of ths $6s\ ^4P_{3/2}$ state by finding the analogous transition in iodine. We find the Einstein A coefficient to be 3×10^6 sec^{-1}; thus it should be possible to see gain on the 1183 Å line of Xe II.

Another scheme which utilizes the idea of recombination is shown in Fig. 10. Here the recombination mechanism provides large storage populations in the lowest metastable level of Kr. During a collision with a Xe ion in the ground state, and in the presence of a laser tuned to the $R = \infty$ wavelength of 9173 Å, energy is selectively transferred to the $5s5p^6\ ^2S_{1/2}$ state of Xe II. Fluorescence is observed on the $5s5p^6\ ^2S_{1/2} \rightarrow 5p^5\ ^2P^o_{1/2}$ transition at 1245 Å. This switched collision system overcomes the problem we have in the Xe-Kr system mentioned earlier — low storage densities. Recent experiments with He and Xe indicate a ^3S population in He of $\sim 10^{14}$ cm^{-3} at a total pressure of $\sim$ 20 torr. Here the Xe is a dopant at the 0.1 - 1.0% level. We expect similar storage densities in the metastable state of Kr. Given high enough storage densities and appropriate lifetimes it may be possible to observe gain at 1245 Å.

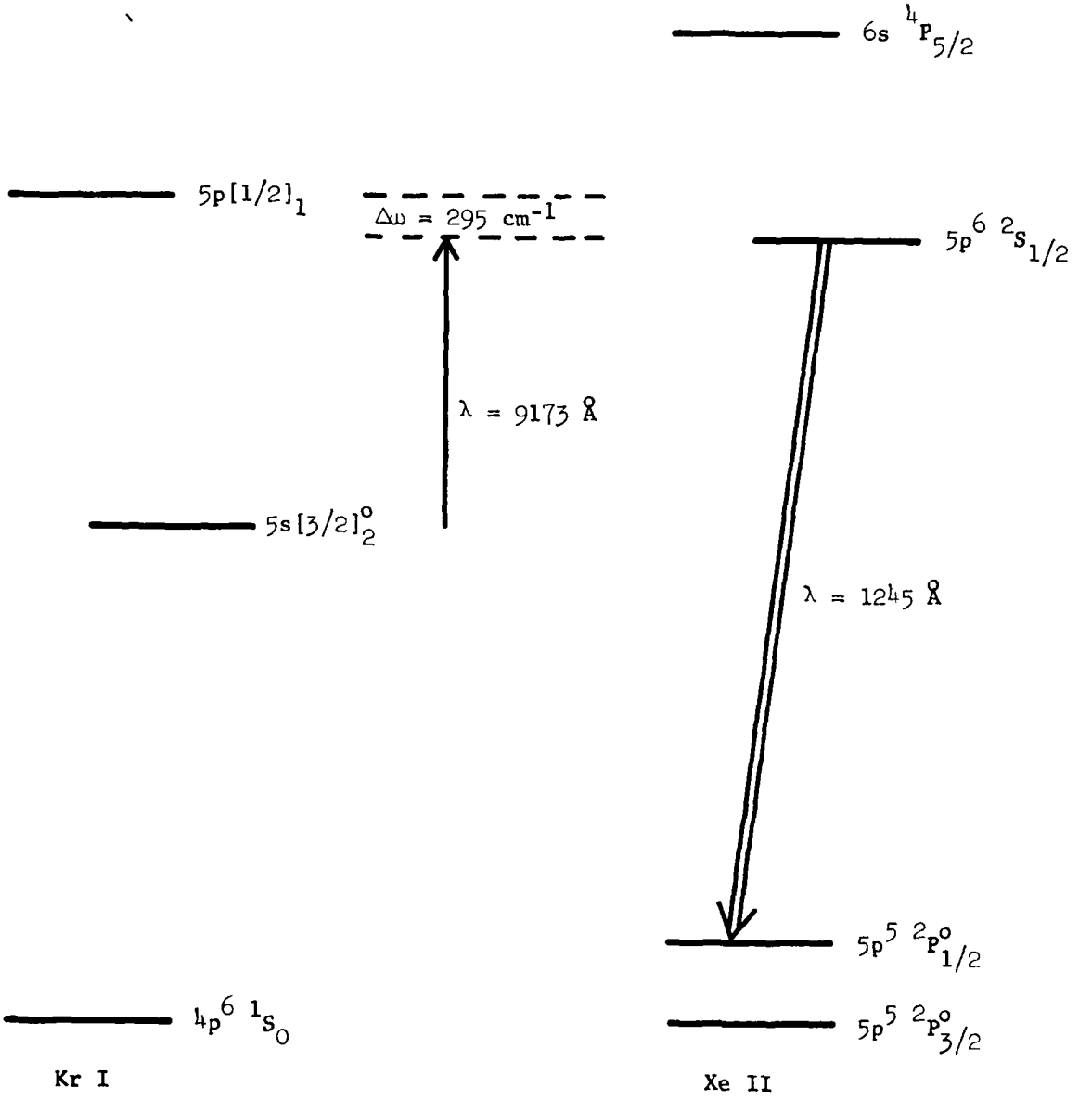

Fig. 10--Kr-Xe laser induced collision.

F. Microwave Excitation of Rare-Gas Halide Lasers

(A. J. Mendelsohn)

Approximately one-half way through the contract period we initiated a project to study the possibility of using rf heated plasmas as an excitation mechanism for rare-gas halide lasers. This idea developed from our theoretical and experimental work on such plasmas for possible extreme VUV and soft x-ray light sources funded by the Office of Naval Research. Although the expected operating conditions for the two applications are quite different, the theoretical modeling and practical experience are still relevant. Our interest resulted from the documented practical advantages and usefulness of these lasers, combined with a number of apparent advantages of microwave excitation.

Rare-gas halide exciplex lasers are the most efficient visible/UV lasers to date, and over the past five years substantial efforts have been made to develop and understand these systems. Efficient excitation of the exciplexes has been achieved with electron beam pumping, electron beam sustained discharges, and UV preionized avalanche electric discharges. In simplistic terms, the function of the excitation mechanism is to efficiently produce large population densities of rare-gas excited states and ions by inelastic collisions with electrons of 5 to 8 eV energy. Following this production there are a number of kinetic channels available leading to the formation of the exciplex lasing species with near-unity efficiency.

All the exciplexes listed in Table 3 have been made to lase by relativistic e-beam pumping, the best results being 12 J/ℓ extraction at 9% intrinsic efficiency for KrF^*. The term "intrinsic efficiency" refers to

Table 3

Rare-Gas Halide Exciplex Lasers

Exciplex	Wavelength (nm)
ArF^*	193
KrF^*	249
$KrC\ell^*$	222
XeF^*	351
$XeC\ell^*$	308
$XeBr^*$	282

the ratio of laser energy extracted to the excitation energy absorbed by the gas mixture. Thus, since much of the e-beam energy is not absorbed in the usual geometry, the true efficiency is much lower. However, e-beam excitation has the advantage that the mechanism for producing the exciting electrons is independent of, and external to, the laser medium and no instabilities or time limitations exist.

The other two conventional excitation methods rely on a pulsed dc electric field across electrodes in the gas to create and/or heat the exciting electron population. In these cases there are two primary competing mechanisms which determine the time evolution of the electron population, and thus the current and voltage characteristics of the discharge. Electrons are produced by ionizing collisions of hot electrons and rare-gas atoms leading to an exponential increase in electron population density and plasma conductivity. This avalanche terminates when the conductivity becomes so high — either overall or in a local instability (arc) — that the excitation source can no longer supply sufficient current to maintain the voltage necessary to heat the electrons. The electron production rate is opposed by the electron attachment rate of the halide atoms in the gas. If the halide concentration is sufficiently high the system will not avalanche; any initial or injected electron population will decay in time, the discharge will be quenched, and few exciplexes will be produced.

In the e-beam sustained discharges the halide concentration is raised until the avalanche time is longer than the pulse lengths of interest, and an external low energy e-beam injects electrons which are heated by the applied electric field. This method has the potential of being more efficient than pure e-beam pumping if tradeoffs relating discharge stability, exciplex

production efficiency, and the ratio of discharge to e-beam power can be realized. The best results to date are 10 J/ℓ extraction at an intrinsic efficiency of 9.5% in KrF^* with a pulse length of 500 ns.

In the third excitation scheme the halide concentration is lowered so that the discharge is self-sustaining and avalance times are "moderate". The discharge is initiated by UV preionization of the gas, and generally is terminated by instabilities in ~ 30 ns. While this is the simplest system to build, the short effective excitation times limits the efficiency to about 2%. We believe that microwave excitation has the potential for combining the stable, efficient, long pulse operation typical of e-beam sustained discharges with the simplicity of the direct discharge systems.

A schematic of the initial experimental geometry is shown in Fig. 11. rf energy in the primary guide is uniformly (constant watts per unit length) coupled into the secondary guide over a ~ 50 cm length. The laser gas mixture is contained in a dielectric tube centered in this second guide. In the presence of the rf field the initial electrons are heated through near-elastic collisions with the rare gas, gaining a small amount of energy in each collision until they are sufficiently hot to create excited states, ions, and more electrons. As the electron population increases the plasma conductivity and absorption increase, leading to efficient utilization of the applied rf energy — as opposed to a shorting out of a dc excitation source. At higher electron densities the dielectric constant of the plasma begins to exceed one significantly and the rf field is unable to penetrate the plasma. The behavior of the system beyond this point is not well characterized because of the unknown influences of such factors as electron diffusion, electron losses at the walls, recombination, and the reduced

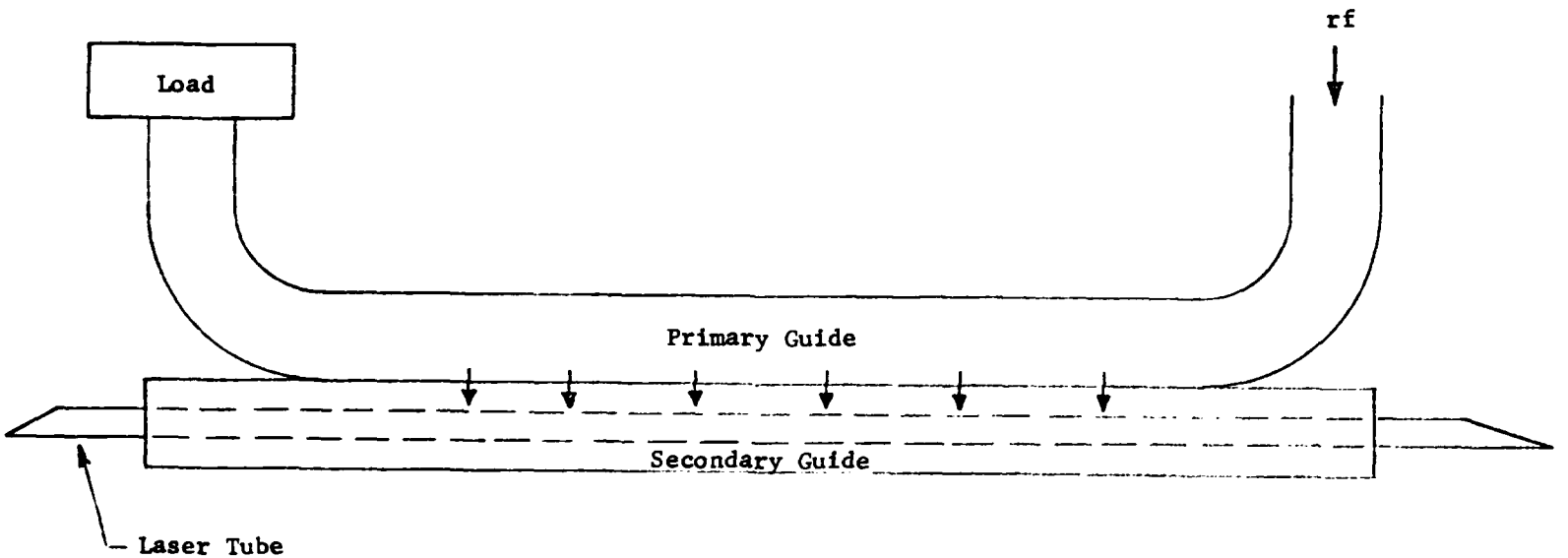

Fig. 11--Microwave periodic coupler.

heating rate. But even if heating does stop completely at this point it will be isotropic, gradual, and non-catistrophic. The time scale of the process can be adjusted, as explained before, by the halide concentration.

The basic advantage of the microwave excitation relative to dc discharges (in addition to the basic stability) is illustrated in Fig. 12. For the 100 MHz quasi-dc case the plasma dielectric constant begins to deviate significantly from one at $n_e \approx 10^{12}$ cm^{-3}, while for our 10 GHz conditions densities 100 times higher are possible before the fields are rejected by the plasma. This translates directly into higher exciplex production rates. Our preliminary calculations show that the microwave heated plasma should create 10^{14} cm^{-3} electrons at a mean temperature of ~ 5 eV, sufficiently hot to allow efficient formation of exciplexes. For the 249 nm KrF^* line we estimate a laser threshold pump power density of ~ 6×10^4 W/cm^3 which is well within the capabilities of our generating equipment.

To date our efforts have been concentrated on the theoretical understanding of the heating and on assembling the initial experiment. Because of the hazardous nature of the halide fraction of the mixture, considerable effort has been expended on building suitable gas handling systems, exhaust hoods, etc. Because of the short absorption lengths (< 1 cm) for microwaves at the high operating pressure (1-2 atm) of excimer lasers, we have devised a coupling structure to feed the microwaves uniformly into the laser medium. The coupler (Fig. 13) is based on the "Riblet-Tee" slot, with the spacing of the individual coupling elements varied along the length to give uniform distribution of the incident power along the laser tube. The coupling structure has been built and performs as expected.

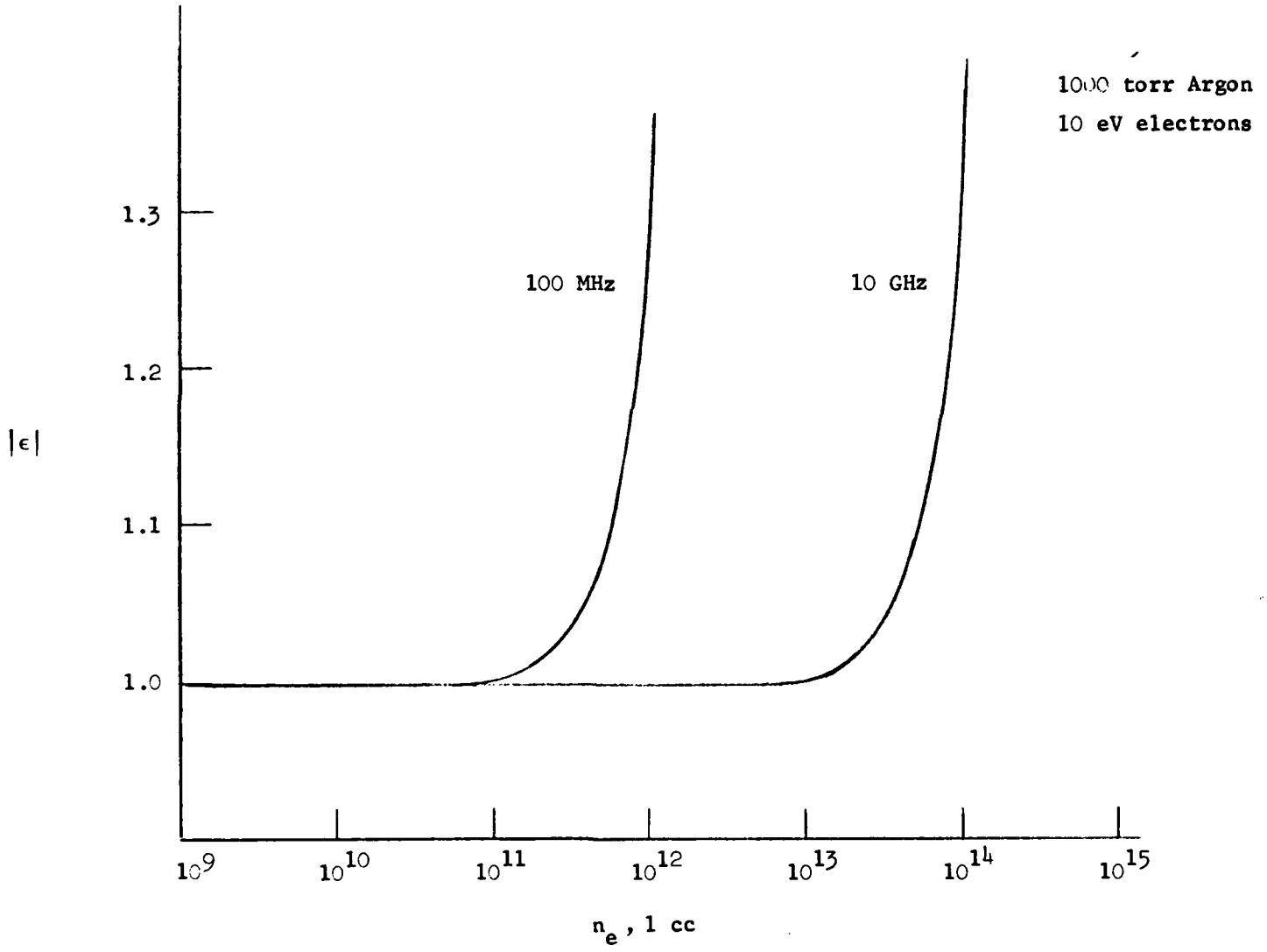

Fig. 12--Plasma dielectric constant.

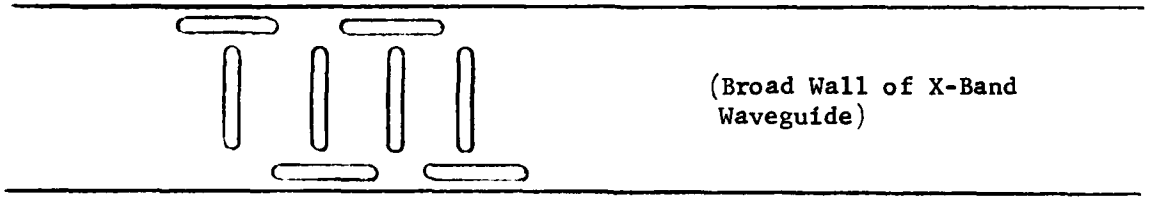

Fig. 13--Detail of "Ribler-Tee" Section.

Our present 10 GHz magnetron is capable of delivering about 0.5 MW, 2 μs long pulses at 400 Hz to the coupler, for an average power of 400 W. Thus laser powers of from 4 to over 20 W should be possible. S-band magnetrons having about ten times greater average power are still realistic laboratory systems, raising the possibility of very high power excimer lasers. The realization of such high average powers, however, may depend critically on developing appropriate gas flow/handling systems and microwave structures. Too little information is presently available on this aspect of excimer laser operation to make even speculative predictions. In practice it is necessary to use high velocity (greater than 1 complete gas exchange per shot) closed cycle gas flow systems incorporating filters and heat exchangers for high average power discharge systems. The underlying reasons for this necessity are not known, although the symptoms without the flow are erratic and unstable discharge conditions. Because of the much greater inherent stability and insensitivity of the microwave discharge relative to the dc case, it is reasonable to expect less of a problem. If the primary factor is gas heating, the expected higher efficiencies of the microwaves should further reduce the problem; if ions sputtered off the electrodes are causing the problem, the absence of electrodes in the rf case may be crucial; and if the instabilities are due to residual electron populations, the greater tolerance of the microwave plasma for high electron densities and its immunity to local catastrophic fluctuations (arcs) appears hopeful.

Even in flowing systems, however, the excimers have a fairly limited lifetime per gas fill. Again, the reasons for the failure are not well known. However, some studies have linked the finite lifetimes to the

formation of optically absorbing species formed by reactions of the halides with sputtered electrode material, and with glass or other insulating ceramics necessary to contain the gas and/or support the electrodes. The microwave discharge technique thus may also yield improved lifetimes. Although our initial design employs a glass or quartz tube, rugged, clean, nonreactive all-metal geometries are possible. We hope that our initial experiments will confirm our basic understanding of the operation of microwave heated discharges, and provide some answers to these difficult practical questions.